Chaos, Solitons & Fractals 66 (2014) 103–119

Contents lists available at ScienceDirect

Chaos, Solitons & Fractals

Nonlinear Science, and Nonequilibrium and Complex Phenomena

journal homepage: www.elsevier.com/locate/chaos

The role of constraints in a segregation model: The symmetric case

Davide Radi [a], Laura Gardini [b,*], Viktor Avrutin [c,b]

[a] Department of Management, Universitá Politecnica delle Marche, Ancona, Italy
[b] DESP, University of Urbino "Carlo Bo", Urbino, Italy
[c] IST, University of Stuttgart, Stuttgart, Germany

ARTICLE INFO

Article history:
Received 2 March 2014
Accepted 25 May 2014
Available online 26 June 2014

ABSTRACT

In this paper we study the effects of constraints on the dynamics of an adaptive segregation model introduced by Bischi and Merlone (2011) [3]. The model is described by a two dimensional piecewise smooth dynamical system in discrete time. It models the dynamics of entry and exit of two populations into a system, whose members have a limited tolerance about the presence of individuals of the other group. The constraints are given by the upper limits for the number of individuals of a population that are allowed to enter the system. They represent possible exogenous controls imposed by an authority in order to regulate the system. Using analytical, geometric and numerical methods, we investigate the border collision bifurcations generated by these constraints assuming that the two groups have similar characteristics and have the same level of tolerance toward the members of the other group. We also discuss the policy implications of the constraints to avoid segregation.

1. Introduction

In his seminal contribution [24], Schelling underlines how discriminatory individual choices can lead to the segregation of two groups of people of opposite kinds. People get separated for different reasons, such as sex, age, income, language or nationality, color of the skin, and the like. Since then, this idea has been developed and tested using mainly an agent-based computer simulation approach, see e.g. [10,32]. Instead [2] introduces an adaptive dynamical model in discrete time that captures the features of the segregation process designed by Schelling. This model is represented by a two-dimensional non invertible map. The analysis of the model provides a rather solid mathematical ground that confirms and extends the qualitative illustration of the dynamics provided by Schelling in [24]. In particular, it shows the possibility, depending on the initial conditions, to end up either in an equilibrium of segregation or in an equilibrium of coexistence of the members of the two groups in the same system. The investigation reveals also more complicated phenomena which could have not been observed in [24] due to the lack of mathematical formalization of the model, such as the emergence of periodic or chaotic solutions. Such oscillatory solutions represent situations in which the number of the members of the two groups that enter or exit the system oscillate perpetually in time as the results of overshooting due to impulsive (or emotional) behavior of the agents.

Following Schelling's ideas, the authors of [2] introduced in the model two constraints that limit the maximum number of the members of each group allowed to enter the system. This is indeed quite relevant, as the constraints may reflect the policy decision of some state or group. The constraints make the model piecewise differentiable and,

* Corresponding author. Tel.: +39 0722 305568.
E-mail addresses: d.radi@univpm.it (D. Radi), laura.gardini@uniurb.it (L. Gardini), Viktor.Avrutin@ist.uni-stuttgart.de (V. Avrutin).

http://dx.doi.org/10.1016/j.chaos.2014.05.009
0960-0779/© 2014 The Authors. Published by Elsevier Ltd.

from a dynamical point of view, can be responsible for the occurrence of border collision bifurcations. In [2], the effects of these constraints are only marginally analyzed and a deeper investigation is left for further researches. In this paper, following their suggestion we provide a comprehensive description of the effects of these constraints on the dynamics of the model. In particular, we use geometrical, analytical and numerical tools to investigate the nature of the dynamics that can arise when changing the values of these constraints.

Limiting the analysis to a symmetric setting, i.e. assuming that the two populations are of the same size and have the same level of tolerance toward the other type of agents, it emerges that if the two constraints are both sufficiently tight, then an equilibrium of non segregation exists and it is stable, together with two coexisting equilibria of segregation, which are always present and always stable. In particular, the two-dimensional bifurcation diagram reveals that if we relax the limitations to the maximum number of the members of the two populations allowed to enter the system, then for certain initial conditions we first observe a transition from a stable equilibrium of coexistence to stable cycles of any period and subsequently a transition from stable cycles to equilibria of segregation. On the contrary, if the constraints are not fixed equally, for example we limit more the members of the population one to enter the system and less the members of population two and this gap is large enough, as a result we can have either only stable equilibria of segregation or coexistence of a stable periodic solution and stable equilibria of segregation. Thus, it is necessary to impose equal and sufficiently tight constraints on the maximum number of the members of the two populations allowed to enter the system, to have, at least for certain initial conditions, the possibility of convergence to an equilibrium of non segregation.

The dynamics of the model here proposed are particularly interesting from a mathematical point of view as well. Indeed, the model is described by a continuous two-dimensional piecewise differentiable map, with several borders, crossing which the system changes its definition. The dynamics associated with piecewise smooth systems is a quite new research branch, and several papers have been dedicated to this subject in the last decade (see, e.g., [9,33]). Such an increasing interest towards nonsmooth dynamics comes both from new theoretical problems which appear due to the presence of borders and from the wide interest in the applied context. In fact, many models are described by constrained functions, leading to piecewise smooth systems, continuous or discontinuous. We recall several oligopoly models with different kinds of constraints considered in the books [22,4], nonsmooth economic models in [7,15,17,23,13], financial market modeling in [8,31,30], and modeling of multiple-choice in [1,12,6].

The map considered in the present paper is characterized by several constraints, leading to several different partitions of the phase plane in which the system changes definition. When an invariant set as a cycle has a periodic point colliding with a border, then a border collision occurs, which often leads to a *border collision bifurcation* (BCB for short), first described in [20] (see also [21,27]). The result of the contact, that is, what happens to the dynamics after the contact, is in general difficult to predict. However, in one-dimensional piecewise smooth systems, the possible results of a generic border collision of an attracting cycle with one border point can be classified depending on the parameters by using the one-dimensional *BCB normal form*, which is the well known skew tent map defined by two linear functions (see, e.g., [16,18,26,27]). This powerful result will be used also in the analysis of the two-dimensional system considered in this work. In fact, the degeneracy of the map in a few regions often leads to a dynamic behavior which is constrained to some one-dimensional set, where the map can be studied by using some suitable one-dimensional restriction, or first return map. Another peculiarity of the degeneracy is that the one-dimensional reduction may be characterized by a flat branch in the shape of the function, leading to *superstable*[1] cycles. For a piecewise smooth map with a flat branch any cycle with a point on that branch is superstable. Examples of systems characterized by a map with a flat branch can be found in [3,11,29,28]. The feature of such systems is that in the parameter space the periodicity regions of superstable cycles are organized according to the well known *U-sequence* (first described in [19], see also [14,28]) which is characteristic for unimodal maps.

The plan of the work is as follows. In Section 2 we introduce the model and describe its main dynamical properties. In Section 3 we analyze the effect of the constraints on the dynamics of the model. In particular, we investigate the BCBs that occur as the constraints change and we provide the main implications in terms of segregation. In Section 4, we conclude providing some indications for possible further explorations of the dynamics of the model.

2. Model setup and preliminaries

As in [2,24], we assume that individuals are partitioned in two classes C_1 and C_2, say "group 1" and "group 2", of respective numerosity N_1 and N_2 and that each group cares about the type of people in the "system", which following [24] is usually considered to be the "district" they live in.

Moreover, we assume that any individual of group i, $i = 1, 2$, who cannot change the group membership, can observe the ratio of the two types of agents at any moment and decide to move in (out) depending on its own (dis) satisfaction with the observed proportion of opposite type agents to its own type. This degree of (dis) satisfaction is captured, for $i = 1, 2$, by the functions

$$R_i(x_i) = \tau_i\left(1 - \frac{x_i}{N_i}\right) \tag{1}$$

where x_i represents the number of members of group i that are in the system. The function $R_i(x_i)$ gives the maximum ratio of individuals of group j ($j \neq i$) to individuals of group i that x_i members of group i abide and parameter τ_i represents the upper limit of this maximum ratio.

[1] A superstable cycle of a one-dimensional map is a cycle with eigenvalue zero, for a two-dimensional map it is a cycle with two eigenvalues zero.

In other words, the members of a group are assumed to be heterogeneous for what concern their own degree of tolerance towards members of the other group, and the function $R_i(x_i)$ represents the level of tolerance characterizing members of group i. It is worth noting that, as suggested in [24,25], the function $R_i(x_i)$ defines a linear relationship between the maximum ratio of members of group j to members of group i that is tolerated by a fraction $\frac{x_i}{N_i}$ of members of group i. The validity of this function of tolerance has been empirically tested in [5] for problems of racial segregation in some American cities. Although there are some differences among cities and other forms of functions of tolerance could be a valid alternative as well, the empirical analysis suggests that the linear function of tolerance here used provides a good representation of reality.

Given the function $R_i(x_i)$, it follows that the maximum number of agents of group j tolerated by x_i members of group i is given by $x_iR_i(x_i)$. Assuming that agents decide to enter or exist the system according to a myopic adaptive mechanism, at any time t agents of group i will enter the system if $x_j(t)$, the number of members of group j in the system at time t, is below the tolerance threshold $x_i(t)R_i(x_i(t))$, i.e. if $x_i(t)R_i(x_i(t)) > x_j(t)$, and will exit otherwise. In particular the relative variation of agents of group i in the system at a given period of time is modeled as γ_i times the difference $x_i(t)R_i(x_i(t)) - x_j(t)$, where parameter γ_i is named the "*the speed of adjustment*". Thus, the equation giving the number of agents of type i that are in the system at time $t+1$ is the following:

$$\frac{x_i(t+1) - x_i(t)}{x_i(t)} = \gamma_i\left[x_i(t)R_i(x_i(t)) - x_j(t)\right]. \tag{2}$$

Assuming also a restriction on the number of members of group i that are allowed to enter the system, say $0 \leqslant x_i(t) \leqslant K_i$, with $K_i \leqslant N_i$, as a result we obtain the following segregation model, as proposed in [2]. It is described by a continuous two-dimensional piecewise-smooth map $T: R^2_+ \to R^2_+$ given by

$$\begin{aligned}(x_1(t+1), x_2(t+1)) &= T(x_1(t), x_2(t)) \\ &= (T_1(x_1(t), x_2(t)), T_2(x_1(t), x_2(t)))\end{aligned} \tag{3}$$

with

$$T_1(x_1,x_2) = \begin{cases} 0 & \text{if} \quad F_1(x_1,x_2) \le 0 \\ F_1(x_1,x_2) & \text{if} \quad 0 \leqslant F_1(x_1,x_2) \leqslant K_1 \\ K_1 & \text{if} \quad F_1(x_1,x_2) \geqslant K_1 \end{cases} \tag{4}$$

$$T_2(x_1,x_2) = \begin{cases} 0 & \text{if} \quad F_2(x_1,x_2) \le 0 \\ F_2(x_1,x_2) & \text{if} \quad 0 \leqslant F_2(x_1,x_2) \leqslant K_2 \\ K_2 & \text{if} \quad F_2(x_1,x_2) \geqslant K_2 \end{cases} \tag{5}$$

where

$$\begin{aligned} F_1(x_1,x_2) &= x_1[1 - \gamma_1 x_2 + \gamma_1 x_1 R_1(x_1)] \\ F_2(x_1,x_2) &= x_2[1 - \gamma_2 x_1 + \gamma_2 x_2 R_2(x_2)] \end{aligned} \tag{6}$$

We recall that the parameters must satisfy $\gamma_i > 0$, $\tau_i > 0$ and $0 < K_i \leqslant N_i$ $(i = 1, 2)$. It is worth pointing out that the possibility and importance of imposing entry constraints, i.e. to impose $K_i \leqslant N_i$ for $i = 1, 2$, was mentioned also in [24], although the issue was only introduced.

From the definition of the map we have that the phase plane of the dynamical system can be divided into several regions where the system is defined by different functions. On the boundaries of the regions the map is continuous but not differentiable. The boundaries of non-differentiability are given by the curves $F_i(x_1,x_2) = K_i$ which can be written in explicit form as follows:

$$\begin{aligned} BC_{1,K}: x_2 &= \left[1 + \gamma_1 x_1 R_1(x_1) - \frac{K_1}{x_1}\right] \Big/ \gamma_1 \text{ where } F_1(x_1,x_2) = K_1 \\ BC_{2,K}: x_1 &= \left[1 + \gamma_2 x_2 R_2(x_2) - \frac{K_2}{x_2}\right] \Big/ \gamma_2 \text{ where } F_2(x_1,x_2) = K_2 \end{aligned} \tag{7}$$

and the solutions of $F_i(x_1,x_2) = 0$ which, as it is immediate, are satisfied by $x_i = 0$, and the points belonging to the curves given by:

$$\begin{aligned} BC_{1,0}: x_2 &= [1 + \gamma_1 x_1 R_1(x_1)]/\gamma_1 \text{ where } F_1(x_1,x_2) = 0, \quad x_1 \neq 0 \\ BC_{2,0}: x_1 &= [1 + \gamma_2 x_2 R_2(x_2)]/\gamma_2 \text{ where } F_2(x_1,x_2) = 0, \quad x_2 \neq 0 \end{aligned} \tag{8}$$

In Fig. 1(a) these four curves are shown for parameter values $\gamma_1 = \gamma_2 = 1$, $\tau_1 = \tau_2 = 4$, $N_1 = N_2 = 1.5$, $K_1 = 1.4$ and $K_2 = 1.1$. In the present work all the figures are shown with the values of γ_i, τ_i and N_i for $i = 1, 2$ as in Fig. 1, while are let to vary the values of the parameters K_1 and K_2, which are the constraints and are responsible for several border collision bifurcations.

The positive quadrant of the phase plane is thus partitioned in nine regions, in each of which a different definition (i.e. a different function) is to be applied. Let us define the regions as follows:

$$\begin{aligned} \Omega_1 &= \{(x_1,x_2) | 0 \leqslant F_1(x_1,x_2) \leqslant K_1 \text{ and } 0 \leqslant F_2(x_1,x_2) \leqslant K_2\} \\ \Omega_2 &= \{(x_1,x_2) | F_1(x_1,x_2) \le 0 \text{ and } 0 \leqslant F_2(x_1,x_2) \leqslant K_2\} \\ \Omega_3 &= \{(x_1,x_2) | F_1(x_1,x_2) \le 0 \text{ and } F_2(x_1,x_2) \le 0\} \\ \Omega_4 &= \{(x_1,x_2) | F_1(x_1,x_2) \le 0 \text{ and } F_2(x_1,x_2) \geqslant K_2\} \\ \Omega_5 &= \{(x_1,x_2) | F_1(x_1,x_2) \geqslant K_1 \text{ and } 0 \leqslant F_2(x_1,x_2) \leqslant K_2\} \\ \Omega_6 &= \{(x_1,x_2) | F_1(x_1,x_2) \geqslant K_1 \text{ and } F_2(x_1,x_2) \le 0\} \\ \Omega_7 &= \{(x_1,x_2) | F_1(x_1,x_2) \geqslant K_1 \text{ and } F_2(x_1,x_2) \geqslant K_2\} \\ \Omega_8 &= \{(x_1,x_2) | 0 \leqslant F_1(x_1,x_2) \leqslant K_1 \text{ and } F_2(x_1,x_2) \le 0\} \\ \Omega_9 &= \{(x_1,x_2) | 0 \leqslant F_1(x_1,x_2) \leqslant K_1 \text{ and } F_2(x_1,x_2) \geqslant K_2\} \end{aligned} \tag{9}$$

so that the map in each region is given by:

$$\begin{aligned} (x_1,x_2) \in \Omega_1 &: (x_1',x_2') = (F_1(x_1,x_2), F_2(x_1,x_2)) \\ (x_1,x_2) \in \Omega_2 &: (x_1',x_2') = (0, F_2(x_1,x_2)) \\ (x_1,x_2) \in \Omega_3 &: (x_1',x_2') = (0,0) \\ (x_1,x_2) \in \Omega_4 &: (x_1',x_2') = (0,K_2) \\ (x_1,x_2) \in \Omega_5 &: (x_1',x_2') = (K_1, F_2(x_1,x_2)) \\ (x_1,x_2) \in \Omega_6 &: (x_1',x_2') = (K_1,0) \\ (x_1,x_2) \in \Omega_7 &: (x_1',x_2') = (K_1,K_2) \\ (x_1,x_2) \in \Omega_8 &: (x_1',x_2') = (F_1(x_1,x_2), 0) \\ (x_1,x_2) \in \Omega_9 &: (x_1',x_2') = (F_1(x_1,x_2), K_2) \end{aligned} \tag{10}$$

From the definition of the map it follows that the rectangle

$$D = [0, K_1] \times [0, K_2] \tag{11}$$

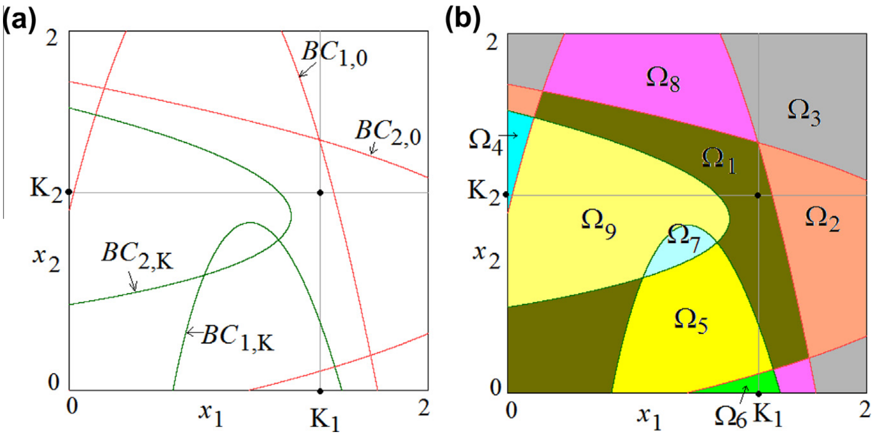

Fig. 1. Parameters: $\gamma_1 = \gamma_2 = 1,\ \tau_1 = \tau_2 = 4$, $N_1 = N_2 = 1.5$, as in all the figures of the paper. $K_1 = 1.4$ and $K_2 = 1.1$. The gray lines mark the border of the phase plane $D = [0, K_1] \times [0, K_2]$. A black dot marks the intersection of these two lines. In (a) the border curves $BC_{1,0}$ and $BC_{2,0}$ in red, the border curves $BC_{1,K}$ and $BC_{2,K}$ in green. In (b) the regions Ω_j of the phase plane are evidenced by different colors. To better clarify the shape of the constraints, we illustrate all the figures in the phase plane $[0, 2] \times [0, 2]$, although the region of interest of the model is $D \subset [0, N_1] \times [0, N_2]$. (For interpretation of the references to colour in this figure legend, the reader is referred to the web version of this article.)

is absorbing, as any point of the plane is mapped in D in one iteration and an orbit cannot escape from it, thus D is our region of interest. In general, depending on the values of the parameters, only a few of the regions Ω_j for $j = 1, \ldots, 9$ may have a portion, or subregion, present in D, say $\Omega_j \cap D \neq \emptyset$, as shown for example in Fig. 1(b). In any case, the behavior of the map in the other regions, not entering D, may be easily explained. To this purpose, let us introduce first a few remarks on the fixed points that the system can have.

The fixed points of the system, satisfying $T(x_1, x_2) = (x_1, x_2)$, are associated with the solutions of several equations. For sure we have some fixed points on the axes, which correspond to disappearance (i.e. extinction) of one population. From $F_i(0, 0) = (0, 0)$ for $i = 1, 2$ we have that the origin $(0, 0)$ is always a fixed point. As we shall see, it is locally unstable. However, due to the constraints, all the points belonging to region Ω_3 are mapped into the fixed point in the origin in one iteration.

The axes are invariant, as considering a point $(x_1, 0)$ on the x_1 axis we have that $T(x_1, 0) = (T_1(x_1, 0), T_2(x_1, 0)) = (T_1(x_1, 0), 0)$ still belongs to the x_1 axis, and

$$T_1(x_1, 0) = \begin{cases} 0 & \text{if} \quad F_1(x_1, 0) \le 0 \\ F_1(x_1, 0) & \text{if} \quad 0 \leqslant F_1(x_1, 0) \leqslant K_1 \\ K_1 & \text{if} \quad F_1(x_1, 0) \geqslant K_1 \end{cases} \tag{12}$$

where

$$F_1(x_1, 0) = x_1\left[1 + \gamma_1 x_1 \tau_1\left(1 - \frac{x_1}{N_1}\right)\right]. \tag{13}$$

Thus, region Ω_6, whose points are all mapped in $(K_1, 0)$ in one iteration, necessarily has non-empty intersection with the rectangle D, and $(K_1, 0)$ is a fixed point of the map. Moreover, considering the restriction $t_1(x_1) \equiv T_1(x_1, 0)$ we have that $t_1(x_1) = x_1$ is satisfied for $x_1^* = 0$ which is a fixed point (representing the origin), and $x_1 = N_1$ which is virtual for $K_1 < N_1$ (constraint that we consider in the model). Thus the map $x_1(t+1) = t_1(x_1(t))$ has a fixed point $x_1^* = K_1$ where the piecewise smooth function $t_1(x_1)$ has a flat branch, which means that the fixed point $(K_1, 0)$ always exists (and it is superstable for the restriction on the axis). While considering $\frac{d}{dx_1} t_1(x_1) = 1 + 2\gamma_1\tau_1 x_1 - 3\frac{\gamma_1\tau_1}{N_1} x_1^2$ we have $\frac{d}{dx_1} t_1(0) = 1$, and $\frac{d^2}{d^2x_1} t_1(x_1) = 2\gamma_1\tau_1 - 6\frac{\gamma_1\tau_1}{N_1} x_1$ leads to $\frac{d^2}{d^2x_1} t_1(0) = 2\gamma_1\tau_1 > 0$ so that the fixed point $x_1^* = 0$ is repelling on its right side, that is, the origin $(0, 0)$ is repelling along the x_1 direction.

Similarly for the second axis, we have that $T(0, x_2) = (T_1(0, x_2), T_2(0, x_2)) = (0, T_2(0, x_2))$ with

$$T_2(0, x_2) = \begin{cases} 0 & \text{if} \quad F_2(0, x_2) \le 0 \\ F_2(0, x_2) & \text{if} \quad 0 \leqslant F_2(0, x_2) \leqslant K_2 \\ K_2 & \text{if} \quad F_2(0, x_2) \geqslant K_2 \end{cases} \tag{14}$$

where

$$F_2(0, x_2) = x_2\left[1 + \gamma_2 x_2 \tau_2\left(1 - \frac{x_2}{N_2}\right)\right]. \tag{15}$$

So region Ω_4 (whose points are all mapped in $(0, K_2)$ in one iteration) intersects the rectangle D and $(0, K_2)$ is a superstable fixed point of the restriction, while the origin $(0, 0)$ is repelling along the x_2 direction. The proof is the same as the one given above for the x_1 axis. Regarding our example, the one-dimensional map $x_2(t+1) = t_2(x_2(t)) \equiv T_2(0, x_2(t))$ is shown in Fig. 2a.

Other comments regarding the fixed points $(K_1, 0)$ and $(0, K_2)$ for the two-dimensional map T will be given below. Here we notice that other fixed points (x_1^*, x_2^*) may exist as solutions of the equations

$$\begin{cases} x_1 R_1(x_1) = x_2 \\ x_2 R_2(x_2) = x_1 \end{cases}$$

when belonging to region Ω_1 (otherwise they are so-called virtual fixed points). These fixed points are represented in the phase plane by the intersection points of the two reaction curves

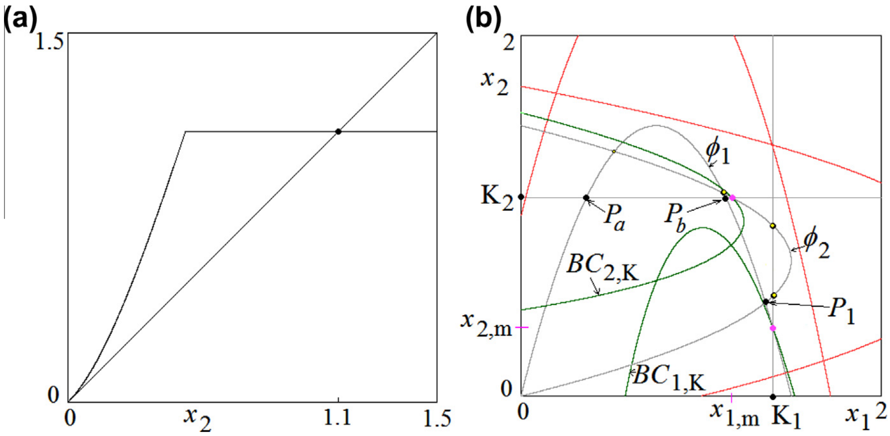

Fig. 2. Parameters as in Fig. 1. In (a) function $t_2(x_2)$ for $x_2 \in [0, N_2]$, the black dot is a superstable equilibrium. In (b) the reaction curves ϕ_1 and ϕ_2, as well as the lines $x_1 = K_1$ and $x_2 = K_2$, are in gray. Black dots are feasible equilibria, black dots with yellow interior are virtual equilibria. The dots in pink are the points $(x_{1,m}, K_2)$ and $(K_1, x_{2,m})$. (For interpretation of the references to color in this figure legend, the reader is referred to the web version of this article.)

$$\phi_1 : \; x_2 = x_1 R_1(x_1) \text{ and } \phi_2 : x_1 = x_2 R_2(x_2) \tag{16}$$

and the number of such points can be at most four.

Moreover, also fixed points (K_1, x_2^*) may exist, associated with the solutions of the equation $x_2 R_2(x_2) = K_1$, when belonging to the region $\Omega_5 \cap D$. Also these fixed points can be graphically seen in the phase plane as intersection points of the two curves $x_1 = K_1$ (vertical straight line) and ϕ_2. Similarly, fixed points of type (x_1^*, K_2) associated with the solutions of the equation $x_1 R_1(x_1) = K_2$ (intersection points of the horizontal straight line $x_2 = K_2$ and ϕ_1) may exist, when belonging to the region $\Omega_9 \cap D$.

The fixed points of the example shown in Fig. 1 are evidenced in Fig. 2(b) where the two curves ϕ_1 and ϕ_2 (having a unimodal shape) are drawn, together with the straight lines $x_1 = K_1$ and $x_2 = K_2$. Besides in the origin, the curves ϕ_1 and ϕ_2 have three intersection points, but two of them belong to the region Ω_9 and are outside D, while the third one, say P_1, belongs to the region Ω_1 in D and thus it is a true fixed point of the map. On the vertical line $x_1 = K_1$ a fixed point is $(K_1, 0)$ on the axis and, as we shall see, it is superstable. Then two more solutions of $x_2 R_2(x_2) = K_1$ exist, but both points belong to the region Ω_1 and thus are virtual fixed points. Differently, on the horizontal line $x_2 = K_2$, besides the superstable fixed point $(0, K_2)$ on the vertical axis, there are two more fixed points of the map, $P_a = (x_{1,a}^*, K_2)$ and $P_b = (x_{1,b}^*, K_2)$, as both belong to the region $\Omega_9 \cap D$. We shall return on these fixed points below.

The definitions of the map in the several regions Ω_j lead to different kinds of degeneracy. For example, when a portion of region Ω_7 exists in D, then all the points of that region are mapped into a unique point: the corner (K_1, K_2) of the absorbing rectangle D, which means that in the region Ω_7 we have two degeneracies, that is, two eigenvalues equal to zero in the Jacobian matrix at any point of Ω_7.

Thus, one more fixed point may be given by the point $P = (K_1, K_2)$ when it belongs to $\Omega_7 \cap D$ (and in such a case this fixed point is superstable: both eigenvalues are equal to zero). While when (K_1, K_2) does not belong to $\Omega_7 \cap D$, then for the dynamics of the points in the region Ω_7 it is enough to consider the trajectory of only one point: (K_1, K_2).

Other regions with double degeneracies are Ω_3, Ω_4 and Ω_6 as all of them are mapped into fixed points, $(0,0)$, $(0, K_2)$ and $(K_1, 0)$, respectively. These fixed points do not deserve for other comments apart from their local stability/instability: as we have seen, the origin is unstable while we shall see below (in Property 2) that the two other fixed points on the axes are superstable when Ω_4 and Ω_6 intersect D in a set of positive measure, stable otherwise.

There are other degeneracies which are immediate from the definition of the map, due to the regions bounded by the border curves $BC_{i,K}$ (see Fig. 1(a)). Considering the portion of the phase plane which is bounded by the border curve $BC_{1,K}$, we have that the whole region is mapped onto the line $x_1 = K_1$. Similarly the whole region bounded by the border curve $BC_{2,K}$ is mapped onto the line $x_2 = K_2$. Thus, in both regions we have one degeneracy as the Jacobian matrix in all the points of these regions has one eigenvalue equal to zero. As a whole region is mapped into a segment of straight line, the dynamics can be associated with the points of those particular segments. In particular, the stability/instability of the fixed points belonging to these lines can be investigated considering the restriction of the map to these lines, when the points belong to the proper region (that is, when they are real fixed points of T and not virtual). Let us first notice the following

Property 1. *The three curves $x_2 = K_2$, $BC_{2,K}$ and ϕ_2 all intersect in the point $(x_{1,m}, K_2)$, where $x_{1,m} = K_2 \tau_2 \left(1 - \frac{K_2}{N_2}\right)$. The three curves $x_1 = K_1$, $BC_{1,K}$ and ϕ_1 all intersect in the point $(K_1, x_{2,m})$, where $x_{2,m} = K_1 \tau_1 \left(1 - \frac{K_1}{N_1}\right)$.*

Proof. In fact, $x_2 = K_2$ intersects $BC_{2,K} : x_1 = \left[1 + \gamma_2 x_2 R_2(x_2) - \frac{K_2}{x_2}\right] / \gamma_2$ in the point $x_{1,m} = K_2 R_2(K_2) = K_2 \tau_2 \left(1 - \frac{K_2}{N_2}\right)$, and also $x_2 = K_2$ intersects $\phi_2 : x_1 = x_2 R_2(x_2) = x_2 \tau_2 \left(1 - \frac{x_2}{N_2}\right)$ in the same point, as it is immediately evident. Similarly for the other curves (these points are evidenced in Fig. 2(b)). □

So, let us consider $x_2 = K_2$ and the segment of this line for $x_1 \geqslant 0$ and $x_1 \leqslant x_{1,m}$, where $x_{1,m}$ is defined in Property 1. This segment is mapped into itself, and the dynamics are given (for $0 \leqslant x_1 \leqslant x_{1,m}$) by the one-dimensional map

$$x_1(t+1) = f_1(x_1(t)),\ f_1(x_1) = \begin{cases} 0 & \text{if} \quad F_1(x_1,K_2) \le 0 \\ F_1(x_1,K_2) & \text{if} \quad 0 \leqslant F_1(x_1,K_2) \leqslant K_1 \\ K_1 & \text{if} \quad F_1(x_1,K_2) \geqslant K_1 \end{cases} \tag{17}$$

where

$$F_1(x_1,K_2) = x_1\left[1 - \gamma_1 K_2 + \gamma_1 x_1 \tau_1 \left(1 - \frac{x_1}{N_1}\right)\right] \tag{18}$$

The point $x_1 = 0$ corresponds to the fixed point $(0, K_2)$ of T, and fixed points with positive values internal to the range $[0, K_1]$ are thus associated with the solutions of a quadratic equation, leading to

$$x^*_{1,b,a} = \frac{N_1}{2} \pm \sqrt{\left(\frac{N_1}{2}\right)^2 - \frac{K_2 N_1}{\tau_1}}. \tag{19}$$

Moreover,

$$\frac{d}{dx_1} F_1(x_1,K_2) = 1 - \gamma_1 K_2 + x_1 \gamma_1 \tau_1 \left(2 - \frac{3x_1}{N_1}\right) \tag{20}$$

so that $\frac{d}{dx_1} F_1(0,K_2) = 1 - \gamma_1 K_2 < 1$, which implies that this fixed point is attracting also on the direction of the line (as the derivative is either zero, when the constraint is active, or positive and smaller than 1), and

$$\frac{d}{dx_1} F_1\left(x^*_{1,b,a}, K_2\right) = 1 + 2\gamma_1 K_2 - x^*_{1,b,a}\gamma_1\tau_1$$
$$= 1 + 2\gamma_1 K_2 - \gamma_1 \tau_1 \left(\frac{N_1}{2} \pm \sqrt{\left(\frac{N_1}{2}\right)^2 - \frac{K_2 N_1}{\tau_1}}\right).$$

Summarizing, the two solutions in (19) lead to fixed points of the two-dimensional map only if $x^*_{1,a} \leqslant x_{1,m}$ and $x^*_{1,b} \leqslant x_{1,m}$ (as it occurs in the example shown in Fig. 2(b)), and their stability depends on the value of $\frac{d}{dx_1} f_1(x_{1,b,a})$. When $|\frac{d}{dx_1} f_1(x_{1,b,a})| < 1$ (resp. > 1) the fixed points are attracting (resp. repelling). In the example considered in Fig. 2(b) both fixed points $P_a = (x^*_{1,a}, K_2)$ and $P_b = (x^*_{1,b}, K_2)$ are repelling.

We can reason similarly for the restriction of the map on the straight line $x_1 = K_1$, for $0 \leqslant x_2 \leqslant x_{2,m}$, where $x_{2,m}$ is defined in Property 1, which is given by the one-dimensional map

$$x_2(t+1) = f_2(x_2(t)),\ f_2(x_2) = \begin{cases} 0 & \text{if} \quad F_2(K_1,x_2) \le 0 \\ F_2(K_1,x_2) & \text{if} \quad 0 \leqslant F_2(K_1,x_2) \leqslant K_2 \\ K_2 & \text{if} \quad F_2(K_1,x_2) \geqslant K_2 \end{cases} \tag{21}$$

where

$$F_2(K_1,x_2) = x_2\left[1 - \gamma_2 K_1 + \gamma_2 x_2 \tau_2 \left(1 - \frac{x_2}{N_2}\right)\right]. \tag{22}$$

Thus, besides $x_2 = 0$, which represents the fixed point $(K_1, 0)$, the fixed points are associated with the solutions of a quadratic equation, leading to

$$x^*_{2,b,a} = \frac{N_2}{2} \pm \sqrt{\left(\frac{N_2}{2}\right)^2 - \frac{K_1 N_2}{\tau_2}}$$

moreover

$$\frac{d}{dx_2} F_2(K_1,x_2) = 1 - \gamma_2 K_1 + x_2 \gamma_2 \tau_2 \left(2 - \frac{3x_2}{N_2}\right) \tag{23}$$

so that $\frac{d}{dx_2} F_2(K_1,0) = 1 - \gamma_2 K_1 < 1$, which implies that this fixed point is attracting also on the direction of the line, and

$$\frac{d}{dx_2} F_2(K_1, x^*_{2,b,a}) = 1 + 2\gamma_2 K_1 - x^*_{2,b,a}\gamma_2\tau_2$$
$$= 1 + 2\gamma_2 K_1 - \gamma_2 \tau_2 \left(\frac{N_2}{2} \pm \sqrt{\left(\frac{N_2}{2}\right)^2 - \frac{K_1 N_2}{\tau_2}}\right).$$

These solutions are fixed points of the two-dimensional map only if $x^*_{2,a} \leqslant x_{2,m}$ and $x^*_{2,b} \leqslant x_{2,m}$.

With the parameter values used in the example shown in Fig. 2(b) both the inequalities given above are not satisfied and thus they lead to virtual fixed points.

We can now end the comments on the fixed points on the axes for the two-dimensional map T. In fact, let us consider the point $(0, K_2)$. We have already seen that along the axes $x_1 = 0$ there is a zero eigenvalue, and now we have the eigenvalue along the invariant segment on $x_2 = K_2$. From the definition of the restriction in (17) and (18) it follows that either this point (the origin of the restriction) is superstable (which occurs when Ω_4 intersects D in a set of positive measure), or stable, as we have $0 < \frac{d}{dx_1} F_1(0, K_2) < 1$. Similarly we can reason for the other fixed point $(K_1, 0)$. This leads to an important property of the model: the two single "segregation states" always exist and attract some points of the phase plane. How many points depends on the structure of the basins of attraction of these fixed points, and on the existence of other attracting sets having states with positive values (not converging to the axes). However, some results are already known from the remarks written above: as all the points of the region Ω_2 are mapped into the x_2 axis, which is trapping and on which we know there is convergence to the fixed point $(0, K_2)$, so we can immediately conclude that all the points of region Ω_2 belong to the basin of attraction of $(0, K_2)$. Similarly, all the points of region Ω_8 belong to the basin of attraction of the fixed point $(K_1, 0)$. We shall see some examples below. We can so state the following

Property 2. *Two stable fixed points always exist in map T given in (3): $(0, K_2)$ and $(K_1, 0)$. The points of the region Ω_4 are mapped into $(0, K_2)$ and those of the region Ω_2 converge to $(0, K_2)$. If $\Omega_4 \cap D$ has a positive measure, then $(0, K_2)$ is superstable for the two-dimensional map T. The points of the region Ω_6 are mapped into $(K_1, 0)$, and those of the region Ω_8 converge to $(K_1, 0)$. If $\Omega_6 \cap D$ has a positive measure, then $(K_1, 0)$ is superstable for the two-dimensional map T.*

In the example considered in Figs. 1 and 2 the two fixed points $(K_1, 0)$ and $(0, K_2)$ on the axes are superstable for map T. Besides them, map T has two more fixed points

$P_a = (x^*_{1,a}, K_2)$ and $P_b = (x^*_{1,b}, K_2)$ in the region $\Omega_9 \cap D$ which are unstable, and one more fixed point $P_1 \in \phi_1 \cap \phi_2$ belonging to the region $\Omega_1 \cap D$. At P_1 the map is smooth $(x_1(t+1), x_2(t+1)) = (F_1(x_1(t), x_2(t)), F_2(x_1(t), x_2(t)))$, and the stability of this fixed point depends on the eigenvalues of the Jacobian matrix evaluated at P_1. In our example also this fixed point P_1 is unstable. The unstable fixed points P_1 and P_a belong to the frontiers separating the basins of attraction. Besides the fixed points of segregation on the axes, a third attracting set exists, as shown in Fig. 3(a).

A trajectory on this chaotic attractor consist of points which alternate from region Ω_9 to the region Ω_1. This may be of great help as the dynamics of T can thus be investigated by use of a one dimensional map: the first return map on a segment of the straight line $x_2 = K_2$. In fact, the points of the attracting set belonging to the region Ω_9 are mapped on the line $x_2 = K_2$ above the point $x_{1,m} = K_2\tau_2\left(1 - \frac{K_2}{N_2}\right)$(in the region Ω_1). Thus, a point (x_1, K_2) of the attractor is mapped in $T(x_1, K_2) = (F_1(x_1, K_2), F_2(x_1, K_2)) \in \Omega_9$ and then a second iteration leads to $T^2(x_1, K_2) = (F_1(F_1(x_1, K_2), F_2(x_1, K_2)), K_2) =: (G(x_1), K_2) \in \Omega_1$. So it can be investigated by use of the following one-dimensional first return map on $x_2 = K_2$:

$$x_1(t+1) = G(x_1(t)) \tag{24}$$

$$G(x_1) = F_1\left(x_1\left(1 - \gamma_1 K_2 + \gamma_1 x_1 \tau_1\left(1 - \frac{x_1}{N_1}\right)\right),\right.$$
$$\left. K_2\left(1 - \gamma_2 x_1 + \gamma_2 K_2 \tau_2\left(1 - \frac{K_2}{N_2}\right)\right)\right) \tag{25}$$

in the range $x_{1,m} = K_2\tau_2\left(1 - \frac{K_2}{N_2}\right) < x_1 < K_1$. This one-dimensional map, in our example, is shown in Fig. 3(b), evidencing the invariant interval J on which the dynamics seem to be chaotic. Indeed, the fixed point in Fig. 3(b) inside the invariant segment J, which corresponds to an unstable 2-cycle of T, is homoclinic. This invariant segment J corresponds to the segment of the attractor on the straight line $x_2 = K_2$ in Fig. 3(a).

As already remarked in the Introduction, the goal of this paper is to investigate the role of the constraints, which are the values of K_1 and K_2, and represent the upper limit number of individuals of a given group allowed to enter the system. In doing so, here we investigate this in the case in which the two states (groups or populations) represented by x_1 and x_2 are in some way symmetric, as characterized by parameters having the same values. Thus, in the next section we shall consider the parameters $N := N_1 = N_2,\ \tau := \tau_1 = \tau_2$ and $\gamma := \gamma_1 = \gamma_2$. Nevertheless, in piecewise smooth dynamical systems as the present one, the other parameters may also be relevant. This aspect and in particular the investigation of the role of the constraints in the generic case, with different parameter values for the two populations, is left for further studies.

In the next section we shall see a two-dimensional bifurcation diagram which immediately emphasizes the attracting cycles existing as a function of the parameters (K_1, K_2). We shall describe several regions in that parameter plane which lead to interesting dynamic behaviors.

3. BCBs and global analysis of the dynamics

Let us first consider the relevant dynamics occurring as a function of the *control parameters* (K_1, K_2), when the other parameters are fixed (in our representative case at the values considered in the figures of the previous section: $N = 1.5,\ \tau = 4$ and $\gamma = 1$). As in this paper we restrict our analysis to populations with the same characteristics (in the parameters $\gamma_i,\ \tau_i$ and N_i), the bifurcations occurring in the parameters (K_1, K_2) are obviously symmetric, which leads to the following Property:

Property 3 (*Symmetric parameter plane*). *Let* $N := N_1 = N_2,\ \tau := \tau_1 = \tau_2$ *and* $\gamma := \gamma_1 = \gamma_2$. *Let the control parameters have the values* $(K_1, K_2) = (\xi, \eta)$ *and let* $\{(a(t), b(t)),\ t > 0\}$ *be the trajectory associated with the*

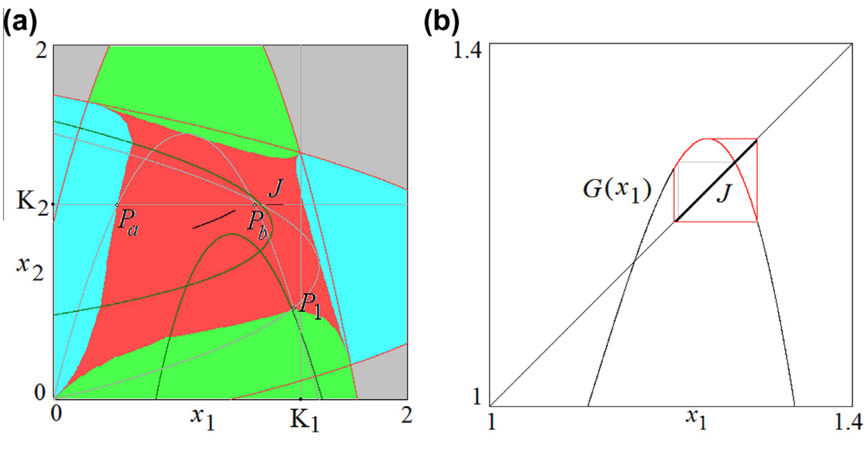

Fig. 3. Parameters as in Fig. 1. In (a) basin of attraction of $(0, K_1)$ in green, basin of attraction of $(0, K_2)$ in azure, basin of attraction of $(0, 0)$ in gray and basin of attraction of the chaotic attractor in red. P_a, P_b and P_1 are unstable equilibria. In (b) first return map $G(x_1)$ on $x_2 = K_2$. J represents an invariant segment, it is the portion of the chaotic attractor of map T that lies on $x_2 = K_2$. The gray lines show that the fixed point of the first return map is homoclinic. (For interpretation of the references to color in this figure legend, the reader is referred to the web version of this article.)

initial condition $(a(0), b(0))$. *Then* $\{(b(t), a(t)),\ t > 0\}$ *is the trajectory associated with the initial condition* $(b(0), a(0))$ *when the control parameters have the values* $(K_1, K_2) = (\eta, \xi)$.

That is, via a change of variable $x_2 := x_1$ and $x_1 := x_2$ we have the same dynamics when K_1 and K_2 are exchanged. This explains the structure, symmetric with respect to the main diagonal, in the two-dimensional bifurcation diagram shown in Fig. 4.

As a particular case of Property 3 we have another property when $K_1 = K_2$ (on the diagonal of the two-dimensional bifurcation diagram of Fig. 4):

Property 4 (*Symmetric phase plane*). *Let* $N := N_1 = N_2$, $\tau := \tau_1 = \tau_2$, $\gamma := \gamma_1 = \gamma_2$ *and* $K := K_1 = K_2$. *Then:*

(4i) *Let* $(a(t), b(t))$ *for any integer* $t > 0$ *be the trajectory associated with the initial condition* $(a(0), b(0))$, *then* $(b(t), a(t))$ *for any integer* $t > 0$ *is the trajectory associated with the initial condition* $(b(0), a(0))$.

(4ii) *On the diagonal* Δ *of the phase plane map* T *reduces to a one-dimensional system. From initial conditions* $x_1(0) = x_2(0)$ *it will be* $x_1(t) = x_2(t)$ *for any integer* $t > 0$ *and the iterates are given by the one-dimensional map defined as* $x(t+1) = T_\Delta(x(t))$ *with*

$$T_\Delta(x) = \begin{cases} 0 & \text{if} \quad F_\Delta(x) \le 0 \\ F_\Delta(x) & \text{if} \quad 0 \leqslant F_\Delta(x) \leqslant K \\ K & \text{if} \quad F_\Delta(x) \geqslant K \end{cases} \tag{26}$$

where $x \equiv x_1 = x_2$ *and* $F_\Delta(x) \equiv F_1(x, x) = F_2(x, x)$ *is given by*

$$F_\Delta(x) = x\left[1 - \gamma x + \gamma x \tau\left(1 - \frac{x}{N}\right)\right]. \tag{27}$$

Clearly, for the points of the phase plane outside the diagonal $x_1 = x_2$ the Property (4i) stated above holds. Moreover, it is worth noting that Property (4i) implies that an invariant set of the two-dimensional map is either symmetric with respect to the diagonal Δ $(x_1 = x_2)$ of the phase plane, or the symmetric invariant set of it also exists.

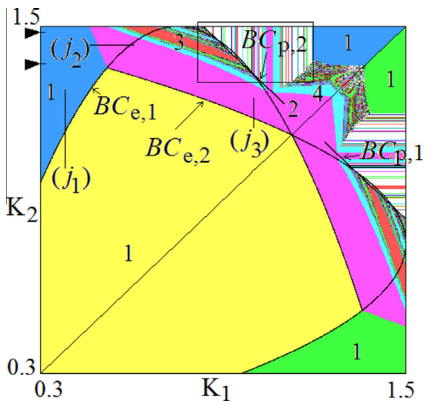

Fig. 4. Two dimensional bifurcation diagram in the (K_1, K_2)-parameter plane for the map T. Different colors are related to attracting cycles of different periods $n \le 30$, the white region corresponds either to chaotic attractors or to cycles of higher periodicity. (For interpretation of the references to color in this figure legend, the reader is referred to the web version of this article.)

As an example let us show the possible bifurcations occurring in the parameter plane of the control parameters (K_1, K_2) in the range $[0, N_1] \times [0, N_2]$ as reported in Fig. 4. As the model is symmetric Property (4i), we can just analyze the dynamics of the model for $K_2 \geqslant K_1$. In Fig. 4 we highlight some BCB curves, which we shall explain below.

It is worth to note that as the parameters K_1 and K_2 influence the borders of the regions at which the piecewise smooth map changes its definition, all the bifurcations that we observe in Fig. 4 are expected to be *border collision bifurcations*. Indeed, even if this is not a sufficient condition to state that all the curves are related to BCBs, the high degeneracy of the map leads to this particular result.

3.1. Case $K_1 = K_2$

Let us first describe the dynamics occurring in the phase plane when the parameters belong to the diagonal $K_1 = K_2$ of the two-dimensional bifurcation diagram, and let $K \equiv K_1 = K_2$. As already shown above, for points in the phase plane belonging to the diagonal where $x \equiv x_1 = x_2$ we can consider the one-dimensional piecewise smooth continuous map $x(t+1) = T_\Delta(x(t))$ (given in (26) and (27)).

The map T_Δ has fixed points satisfying the equation $F_\Delta(x) = x$, leading to a fixed point in $x = 0$ (representing the origin) and $x^* = N(1 - \frac{1}{\tau})$ which exists (positive) only for $\tau > 1$. It is a real fixed point if $N(1 - \frac{1}{\tau}) \leqslant K$, otherwise $x^* = K$ is a fixed point on the flat branch of the function. We can state the following

Property 5. *Let* $N := N_1 = N_2$, $\tau := \tau_1 = \tau_2 > 1$, $\gamma := \gamma_1 = \gamma_2$ *and* $K := K_1 = K_2$.

(5i) *For* $K < N(1 - \frac{1}{\tau})$ *map* T_Δ *has a positive fixed point* $x^* = K$ *belonging to a flat branch, while for* $K > N(1 - \frac{1}{\tau})$ *map* T_Δ *has a positive fixed point* $x^* = N(1 - \frac{1}{\tau})$ *belonging to a smooth branch. At* $K = N(1 - \frac{1}{\tau})$ *a border collision of the fixed point* x^* *occurs. If the bifurcation value satisfies* $K < \overline{K}$ *(resp.* $K > \overline{K}$*), where*

$$\overline{K} = \frac{2\gamma(\tau - 1)N + \sqrt{(2\gamma(\tau - 1)N)^2 + 24N\gamma\tau}}{6\gamma\tau} \tag{28}$$

then increasing K *the result of the border collision is persistence of a stable fixed point (resp. a repelling fixed point and a superstable 2-cycle with periodic points* $\{K,\ T_\Delta(K)\}$*).*

(5ii) *For* $K > T_\Delta(x_c)$ *where*

$$x_c = \frac{(\tau - 1)N}{3\tau} + \sqrt{\left(\frac{(1 - \tau)N}{3\tau}\right)^2 + \frac{N}{3\gamma\tau}} \tag{29}$$

map T_Δ *is smooth. At* $K = T_\Delta(x_c)$ *there is a transition from piecewise-smooth to smooth.*

Proof. We notice that at $K = N(1 - \frac{1}{\tau})$ for the two-dimensional map T the fixed point undergoes a codimension-two border collision as two borders are crossed simultaneously $(\phi_1$ and $\phi_2)$.

At the bifurcation value $K = N(1 - \frac{1}{\tau})$ the fixed point x^* merges with the border point (a point in which the map changes its definition), so it is a border collision. Increasing the value of K, the fixed point x^* moves from the flat branch to the smooth branch. The result of this collision is completely predictable, as already remarked in the literature (see for example [27] and references therein). In fact, in the one-dimensional case the skew-tent map can be used as a border collision normal form, which means that in general, apart from codimension-two bifurcation cases, the slopes of the two functions on the right and left side of the border point at the BCB parameters values determine which kind of dynamic behavior will appear after the BCB. In our case we have that the slope on the left side of the border point is zero while on the right side it is given by $F'_\Delta(K)$(also $F'_\Delta(K) = F'_\Delta(N(1-\frac{1}{\tau})) = F'_\Delta(x^*)$). Thus if $F'_\Delta(K) > -1$ (as the function is decreasing) we have persistence of a stable fixed point, while if $F'_\Delta(K) < -1$ the fixed point on the smooth branch is unstable and a superstable 2-cycle exists (i.e. with eigenvalue equal to zero). We have

$$F'_\Delta(x) = 1 + 2\gamma(\tau - 1)x - 3\frac{\gamma\tau}{N}x^2$$

so that $F'_\Delta(0) = 1$ and $F''_\Delta(0) = 2\gamma(\tau - 1) > 0$ for $\tau > 1$ leading to $x^* = 0$ repelling on its right side. Moreover,

$$F'_\Delta(K) = 1 + 2\gamma(\tau - 1)K - 3\frac{\gamma\tau}{N}K^2$$

and $F'_\Delta(K) < -1$ for $K > \overline{K}$ where $\overline{K}$ is given in (28). For $K > N(1 - \frac{1}{\tau})$ a superstable 2-cycle appears, with periodic points K and $F_\Delta(K)$.

In our specific example considered in Fig. 4 the qualitative shape of the map is shown in Fig. 5(a), it is $N(1 - \frac{1}{\tau}) = 1.125$, thus for $K < 1.125$ the map has a positive fixed point $x^* = K$. The BCB of the fixed point occurs at $K = 1.125$, and it is $\overline{K} \simeq 1.07$, so that at the bifurcation value we have $K > \overline{K}$ and by Property (5i) a 2-cycle appears.

When the fixed point x^* exists, belonging to the decreasing branch (i.e. after the border collision), from piecewise smooth the map may become smooth. To detect this transition let us consider the critical point x_c of T_Δ (point in which the derivative of F_Δ in (27) vanishes), where x_c is given in (29). Then for $K < T_\Delta(x_c)$ the map T_Δ has a horizontal flat branch (as it occurs in our example in Fig. 5), while for $K \geqslant T_\Delta(x_c)$ the map is smooth (as it occurs in our example for $K = 1.4$). □

Notice that the two border points of the map $T_\Delta(x)$, bounding the flat branch, are given by the solutions of the equation $F_\Delta(x) = K$, that is

$$x\left[1 - \gamma x + \gamma x\tau\left(1 - \frac{x}{N}\right)\right] = K$$

As long as the fixed point $x^* = K$ exists in the flat branch, the two border points are one smaller and one larger than K, while after its BCB (with the largest border point) the two border points are both smaller than K (see Fig. 5).

After the BCB of the fixed point we can consider the second iterate of the map $T^2_\Delta(x)$ which, besides the unstable fixed point $x^* = N(1 - \frac{1}{\tau})$, has a pair of superstable fixed points (related to a 2-cycle) which also undergo a border collision. The BCB of the fixed point of T^2_Δ can be studied in the same way as above for the fixed point of T_Δ. In particular, a sequence of period doubling BCBs (also called flip BCBs) occurs, leading to superstable cycles of period 2^n.

In Fig. 5(a) the fixed point $x^* = K$ is still on the flat branch, while in Fig. 5(b), after its BCB, we have a 2-cycle, and in Fig. 5(c) also the 2-cycle is unstable and a superstable 4-cycle exists, with periodic points K and its first three iterates.

As K increases, all the cycles existing in the complete U-sequence (see [19,14]) appear also here, either by saddle-node BCB or by flip BCB. For $T_\Delta(x)$ the cycles are either superstable or unstable. The superstable cycles occur as long as in the map a flat branch persists, that is, as remarked above in Property (5ii), as long as $K < T_\Delta(x_c)$, in which case the unstable cycles may belong to a chaotic repeller. While for $K > T_\Delta(x_c)$ an invariant chaotic set may exist for the one-dimensional map T_Δ bounded by the critical point $T_\Delta(x_c)$ and its images.

Going back to the two-dimensional map T in the phase plane (x_1, x_2), for $K < T_\Delta(x_c)$ the one-dimensional map $T_\Delta(x)$ is piecewise smooth, and the attracting set for T is some $n-$cycle on Δ having one (and necessarily only one) periodic point belonging to the region Ω_7 and its image is the point (K, K). *It follows that such an $n-$cycle is superstable also for the two-dimensional map T.* However, it is not easy

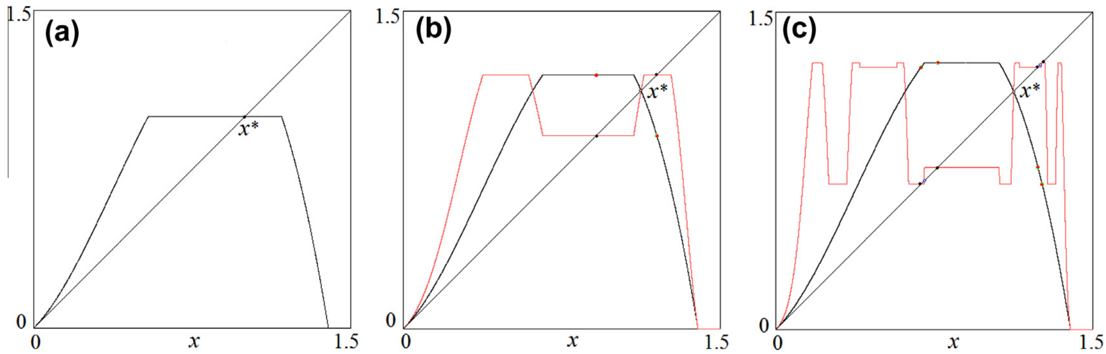

Fig. 5. In (a) map T_Δ at $K = 1$, superstable fixed point $x^* = K$. In (b) map T_Δ and its second iterate at $K = 1.2$, superstable 2-cycle and unstable fixed point x^*. In (c) map T_Δ and its fourth iterate at $K = 1.26$, superstable 4-cycle and unstable fixed point x^*.

to predict the shape of its basin of attraction, as this attractor coexists with the fixed points on the two axes, and other attracting sets may exist in the phase plane outside Δ. For example, for $K = 1.2$, when an attracting 2-cycle exists, its basin of attraction is qualitatively similar to the one shown in Fig. 3(a) for the chaotic attractor. Differently it occurs for $K = 1.2895$, when an attracting 3-cycle exists on the diagonal Δ, but it is not the unique attractor with positive periodic points. In fact, it coexists with an attracting 4-cycle, born in pair with an unstable 4-cycle via saddle-node BCB, and the stable set of the unstable 4-cycle belongs to the frontier of the basins, shown in Fig. 6(a).

In order to investigate the stability and bifurcations of the 4-cycle we notice that, as already performed above, this can be done by use of a one dimensional map: the first return map on the straight line[2] $x_2 = K$ for $x_1 > x_{1,m} = K\tau(1 - \frac{K}{N})$. So doing, it is possible to consider $T^4(x_1, K) = (\psi(x_1), K)$. The one-dimensional first return map $x_1(t+1) = \psi(x_1(t))$ has a stable fixed point in the range $[x_{1,m}, K]$, corresponding to the point Q in Fig. 6(a), with a positive eigenvalue. For increasing K this fixed point undergoes a pitchfork bifurcation, leading to a pair of stable fixed points of T^4 which correspond to two stable 4-cycles for T (see Fig. 6(b)). While the periodic points of the 4-cycles (one stable and one unstable) in Fig. 6(a) are symmetric with respect to Δ, those of the pair of stable 4-cycles existing after the pitchfork bifurcation are not symmetric themselves, but the two cycles have points which are pairwise symmetric with respect to Δ (as stated in Property-(4i)).

We notice that even if we have called the described bifurcation as *pitchfork*, this term is proper only for the one-dimensional first return map on the straight line $x_2 = K$. In fact, let us reason as follows: considering the attracting 4-cycle before the bifurcation (as shown in Fig. 6(a)) we can see that two periodic points are in the region Ω_1, one in the region Ω_5 and one in the region Ω_9. Locally, in each point of the 4-cycle the map is smooth, and intuitively one can expect that the stability/instability of the 4-cycle depends on the eigenvalues of the Jacobian matrix of the map T^4 evaluated in any one of the four fixed points belonging to the 4-cycle of T, and obviously one eigenvalue is expected to be zero, due to the degeneracy of the map in the regions Ω_5 and Ω_9. But this is not correct. The eigenvalue different from zero so determined, is not associated with the bifurcations of the 4-cycle. This is due to the degeneracy of the map: all the points of region Ω_5 are mapped onto the straight line $x_1 = K$ independently on the eigenvalues associated with the smooth map T in points of this line belonging to the region Ω_1. That is: the bifurcation associated with cycles must be determined by using the first return map, as we have done above, and not by using the standard tools which are correct for smooth systems (also locally).

Differently from the case $K < T_\Delta(x_c)$, when a superstable cycles exists for T on the diagonal of the phase plane, for $K > T_\Delta(x_c)$ the one-dimensional map $T_\Delta(x)$ is smooth and an invariant set, which may be chaotic, exists on Δ. However, this invariant set may be not transversely attracting for the two-dimensional map T in the phase plane (x_1, x_2). In fact, this can also be observed in our example at $K = 1.4$: a chaotic interval exists on the diagonal Δ, which is a chaotic repeller in the plane (x_1, x_2), the only attracting sets are the fixed points $(K, 0)$ and $(0, K)$ on the axes, and their basins are separated by a fractal frontier, as shown in Fig. 7 (where the chaotic saddle is also evidenced by a black segment on Δ). This may lead to a significant complexity in the socioeconomic interpretation of the dynamics of the model. Indeed, given a generic value $(x_1(0), x_2(0))$ as initial condition it is hard to predict whether the states are ultimately converging to extinction of the first group or to extinction of the second group.

The analysis conducted till now for $K_1 = K_2$ reveals the importance of the constraints for avoiding segregation. Indeed, from the dynamics of the model we know that if the number of the members of the two populations that are allowed to enter the system is sufficiently small, we always have a stable equilibrium of non segregation. On the contrary, as the maximum number of agents of the two groups that are allowed to enter the system increases, the equilibrium of non segregation loses its stability and a sequence of cycles of different periods appears. Further increasing this limit, we have that only equilibria of segregation are stable. This positive effect of the entry constraints on avoiding segregation can be explained observing that the reaction of agents of one group toward the presence of agents of the opposed group in the system is limited if the presence of the agents of both groups is small in number. In other words, the entry constraints avoid the problem of overshooting, which can be interpreted as impulsive and emotional behaviors.

3.2. Case $K_1 \neq K_2$

Let us first describe some of the BCB curves observable in Fig. 4. The yellow region in the center of the figure is associated with the existence of the superstable fixed point $P = (K_1, K_2) \in \Omega_7$. In our numerical simulations (in the given example) it is the only attractor coexisting with the fixed points on the axes, and its basin of attraction has a shape similar to the one shown in Fig. 3(a) (for the chaotic attractor). The boundaries of the yellow region in the two-dimensional bifurcation diagram in Fig. 4 are clearly curves of BCB, associated with a collision of P with the borders $BC_{1,K}$ and $BC_{2,K}$ given in (7). The condition for the border collision is given by $P \in BC_{1,K}$ and $P \in BC_{2,K}$ leading to the BCB curves having the following equations:

$$BC_{e,1} : K_2 = K_1\tau_1\left(1 - \frac{K_1}{N_1}\right) \text{ at which } P = (K_1, K_2) \in BC_{1,K}$$
$$(30)$$
$$BC_{e,2} : K_1 = K_2\tau_2\left(1 - \frac{K_2}{N_2}\right) \text{ at which } P = (K_1, K_2) \in BC_{2,K}$$

which are drawn in Fig. 4. Notice that the intersection point of these two BCB curves, different from zero, is given by $K_1 = K_2 = N(1 - \frac{1}{\tau})$ which corresponds to the BCB of the fixed point $K = N(1 - \frac{1}{\tau})$ commented in Section 3.1. Let us consider the region with $K_2 > K_1$, see Fig. 4. For parameters

[2] We can use, equivalently, the first return map on the straight line $x_1 = K$.

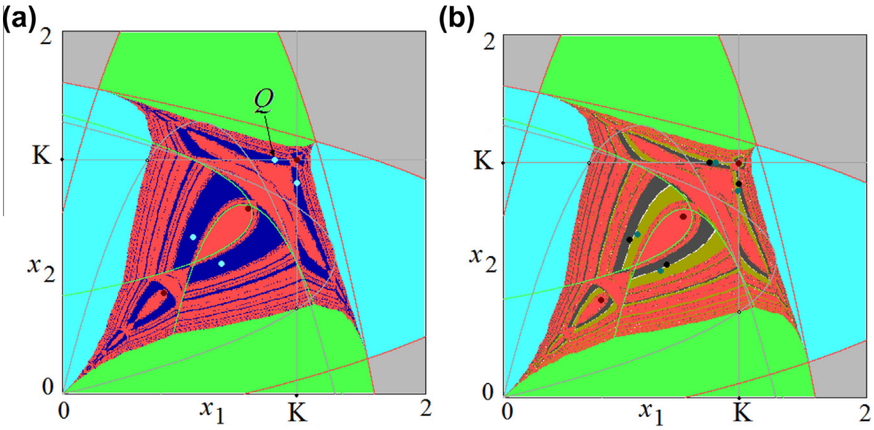

Fig. 6. Basin of attraction of $(K,0)$ in green. Basin of attraction of $(0,K)$ in azure. Basin of attraction of $(0,0)$ in gray. Basin of attraction of the attractor lying on $x_1 = x_2$ in red. In (a) $K = 1.2895$, the blue region is the basin of attraction of the 4-cycle. In (b) $K = 1.29415$, the dark-blue and dark-green regions are the basins of attraction of the two 4-cycles born by pitchfork bifurcation. (For interpretation of the references to color in this figure legend, the reader is referred to the web version of this article.)

in the yellow region the fixed point P is superstable. When a parameter point crosses these curves the fixed point P either disappears by saddle-node BCB, when crossing $BC_{e,1}$, or enters (continuously) region Ω_5 when crossing $BC_{e,2}$. In our example, for parameters crossing $BC_{e,1}$ along the path (j_1) in Fig. 4, the fixed point P merges with the unstable fixed point P_a on the frontier of its basin of attraction and disappears, leaving the two fixed points on the axes as the only attractors. In Fig. 8(a) it is shown the phase plane before the bifurcation, and in Fig. 8b after the bifurcation, when P_a becomes virtual and (K_1, K_2) is no longer a fixed point. It can be seen that after the bifurcation, the former basin of P is included in the basin of $(0, K_2)$.

A similar bifurcation involving a 2-cycle is shown changing the parameters along the path (j_2) in Fig. 4. For low values of K_1 only the two fixed points on the axes are attracting (see Fig. 9(a)). Increasing K_1, a pair of 2-cycles appear by saddle-node BCB. Fig. 9(b) shows the phase plane very close to the bifurcation value, one of the pair of 2-cycles is attracting, with one periodic point in the region Ω_7 and one in the region Ω_1, while the saddle 2-cycle has periodic points in the regions Ω_9 and Ω_1 (see Fig. 9(c)).

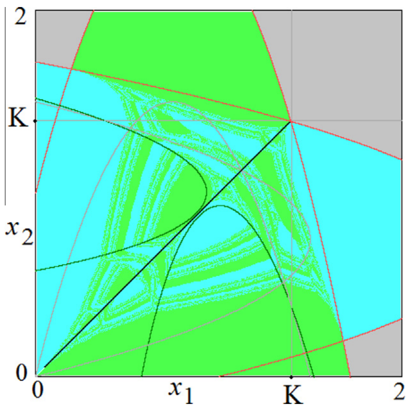

Fig. 7. $K = 1.4$ Basin of attraction of $(K,0)$ in green, basin of attraction of $(0,K)$ in azure, separated by a fractal frontier. The black dots along the line $x_1 = x_2$ belong to a chaotic saddle. (For interpretation of the references to color in this figure legend, the reader is referred to the web version of this article.)

The occurrence of this saddle-node BCB of the 2-cycle can also be determined analytically. In fact, considering the point (K_1, K_2), it must be a fixed point for the second iterate of map T. Thus let

$$F_1(K_1,K_2) = K_1\left[1 - \gamma_1 K_2 + \gamma_1\tau_1 K_1\left(1 - \frac{K_1}{N_1}\right)\right] \tag{31}$$

$$F_2(K_1,K_2) = K_2\left[1 - \gamma_2 K_1 + \gamma_2\tau_2 K_2\left(1 - \frac{K_2}{N_2}\right)\right]$$

the BCB curve satisfies the equation

$$F_1(F_1(K_1,K_2), F_2(K_1,K_2)) = K_1$$

that is:

$$F_1(K_1,K_2)\left[1 - \gamma_1 F_2(K_1,K_2) + \gamma_1\tau_1 F_1(K_1,K_2)\left(1 - \frac{F_1(K_1,K_2)}{N_1}\right)\right] = K_1$$

Notice that in Fig. 4 we have plotted the complete curves $BC_{e,1}$ and $BC_{e,2}$ as also the other parts, not bounding the region of a superstable fixed point, may be related to some border collision. Their effect may also be only of *"persistence border collision"*, as it happens for example along the path (j_2) in Fig. 4: for increasing K_1 the curve $BC_{e,1}$ is crossed, and the stable 2-cycle persists stable, but with periodic points in different regions (one point in Ω_7 and one in the region Ω_9).

In general, in order to predict the effect of a BCB of the fixed point, we can use the first return map along the straight line $x_1 = K_1$ (considering the part above the diagonal in Fig. 4) and then make use of the skew tent map as the border collision normal form, evaluating the slopes of the functions at the border point, at the bifurcation values, as recalled in the previous sections. For example, crossing the curve $BC_{e,2}$ along the path (j_3) in Fig. 4 the fixed point P crosses the curve $BC_{2,K}$ and enters region Ω_5. The fixed

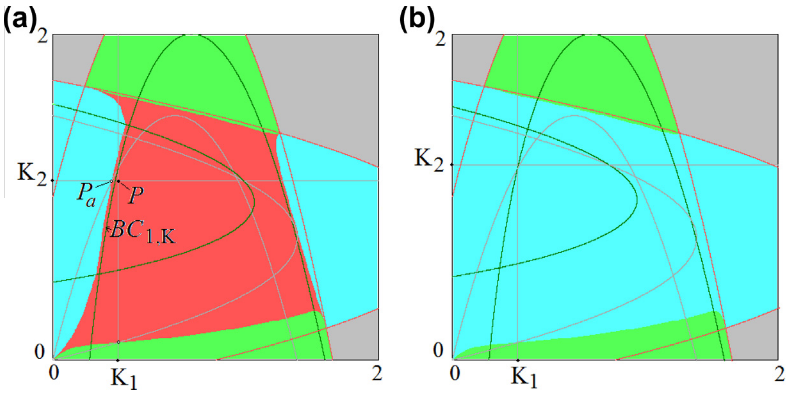

Fig. 8. Bifurcation through (j_1), i.e. $K_1 = 0.4$. In (a) a superstable equilibrium, P, with basin in red, and a saddle, P_a, exist for $K_2 = 1.1$. In (b) for $K_2 = 1.2$ the equilibria P and P_a do not exist anymore as they disappeared by saddle-node BCB increasing K_2. (For interpretation of the references to color in this figure legend, the reader is referred to the web version of this article.)

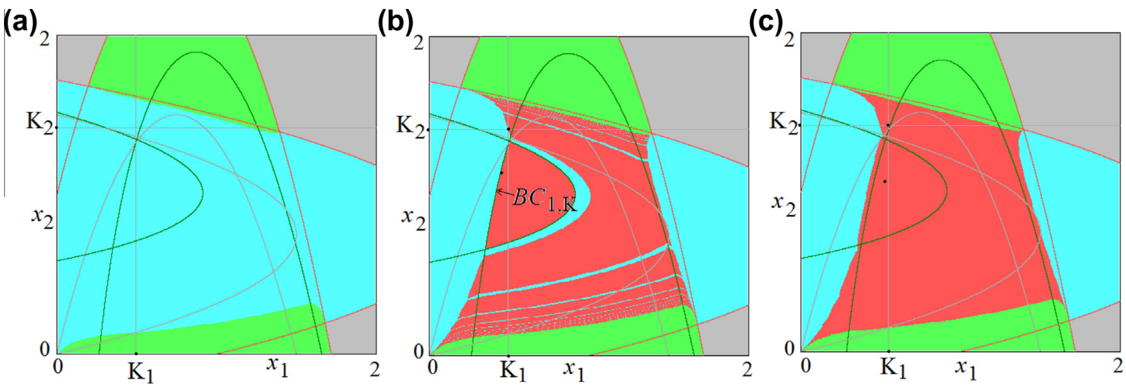

Fig. 9. Bifurcation through (j_2), $K_2 = 1.42$. In (a) $K_1 = 0.4936$. In (b) $K_1 = 0.4937$. In (c) $K_1 = 0.55$. Basin of attraction of the 2-cycle in red. (For interpretation of the references to color in this figure legend, the reader is referred to the web version of this article.)

point becomes unstable and a stable 2-cycle appears, having one periodic point in the region Ω_7 and one in the region Ω_5. In Fig. 10 it is shown the phase plane before the bifurcation, and in Fig. 10(b) the shape of the one-dimensional map restriction of T to the straight line $x_1 = K_1$, for $0 \leqslant x_2 \leqslant x_{2,m}$, given in (21) and (22), showing the superstable fixed point on the horizontal branch. The BCB of P crossing the curve $BC_{2,K}$ in Fig. 10(a) corresponds to the BCB of the fixed point $x_2^* = K_2$ of the 1D map (21) in Fig. 10(b). The slopes at the bifurcation value are one zero and one smaller than -1, thus the fixed point becomes unstable and a sTable 2-cycle appears, as shown in Fig. 10(c) and (d). We can see that the structure of the basins does not change.

Increasing K_2 along the path (j_3) in Fig. 4, the one-dimensional bifurcation diagram is reported in Fig. 11(a). It can be seen that after the 2-cycle, also attracting cycles of period 2^n for any n exist. This can be seen also in the enlargement of Fig. 4 reported in Fig. 11(b). This region of the parameter plane corresponds to a region in which the BCBs lead to the appearance of all stable cycles in accordance with the U-sequence, as already remarked. In fact, the cycles there appearing all have one periodic point in the region Ω_7 and the periodic points either belong all to the straight line $x_1 = K_1$ (in which case the BCB can be studied via the restriction of T on that line) or can be studied via the first return map on that line. All these cycles are superstable for these one-dimensional maps as well as for the two-dimensional map T, and undergo the border collisions. The periodicity regions observable in Fig. 11(b) are ordered according to the U-sequence.

From the enlargement in Fig. 11(b) it can be seen a change in the structure: first (on the left side) the periodicity regions of the superstable cycles exist, and then a region with vertical strips appears. All the regions associated with superstable cycles on the left, according to the U-sequence, also have vertical strips on the right (still according to the U-sequence). This transition, which is typical for one-dimensional piecewise smooth maps with a horizontal branch, corresponds to the loss of the flat branch in the first return map or in the one-dimensional restriction representing the dynamics of the map T. In fact, as recalled above, the restriction of T to the line $x_1 = K_1$ has a horizontal branch as long as the cycles existing in the region characterized by the U-sequence have one periodic point in the region Ω_7. An example

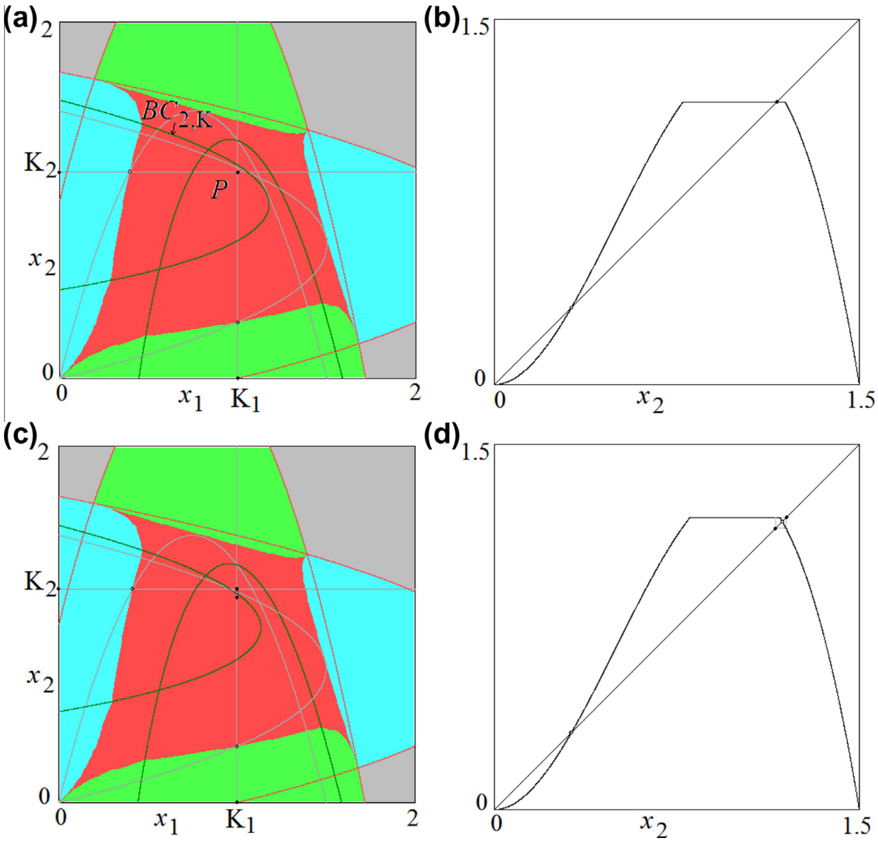

Fig. 10. Bifurcation through (j_3), i.e. $K_1 = 1$. In (a) and (b) $K_2 = 1.16$. In (a) the basin of attraction of $P = (K_1, K_2)$ is in red. In (b) map $f_2(x_2)$ where black dot is the superstable equilibrium $x_2^* = K_2$. In (c) and (d) $K_2 = 1.2$, superstable 2-cycle appeared through a BCB of the fixed point P. In (c) basin of attraction of this 2-cycle in red. In (d) map $f_2(x_2)$ where the black dots are the 2-cycle. In (a) and (c) the black dots with while interior represent unstable equilibria. (For interpretation of the references to color in this figure legend, the reader is referred to the web version of this article.)

is shown in Fig. 10, and in Fig. 12(a) and (b) it is reported the map at the value of K_1 for which there is a superstable 4-cycle. Increasing K_1, a BCB occurs when the restriction of T to the line $x_1 = K_1$ becomes smooth, as shown in Fig. 12(c) and (d).

In order to obtain the bifurcation curves in the parameter space (K_1, K_2), we proceed as follows. As recalled above, the restriction of map T to the line $x_1 = K_1$ is given in (21) and (22). The maximum of the function $F_2(K_1, x_2), \max_{x_2} \{F_2(K_1, x_2)\}$, is obtained considering its proper critical point

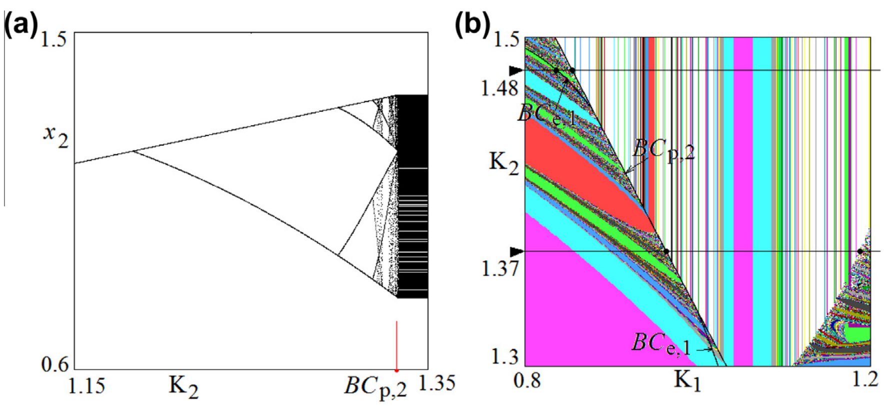

Fig. 11. In (a) 1D bifurcation diagram along (j_3), i.e. $K_1 = 1$, and $K_2 \in [1.15, 1.35]$. The red segment represents the moment in which curve $BC_{p,2}$ is crossed. In (b) enlargement of the rectangle shown in Fig. 4. (For interpretation of the references to color in this figure legend, the reader is referred to the web version of this article.)

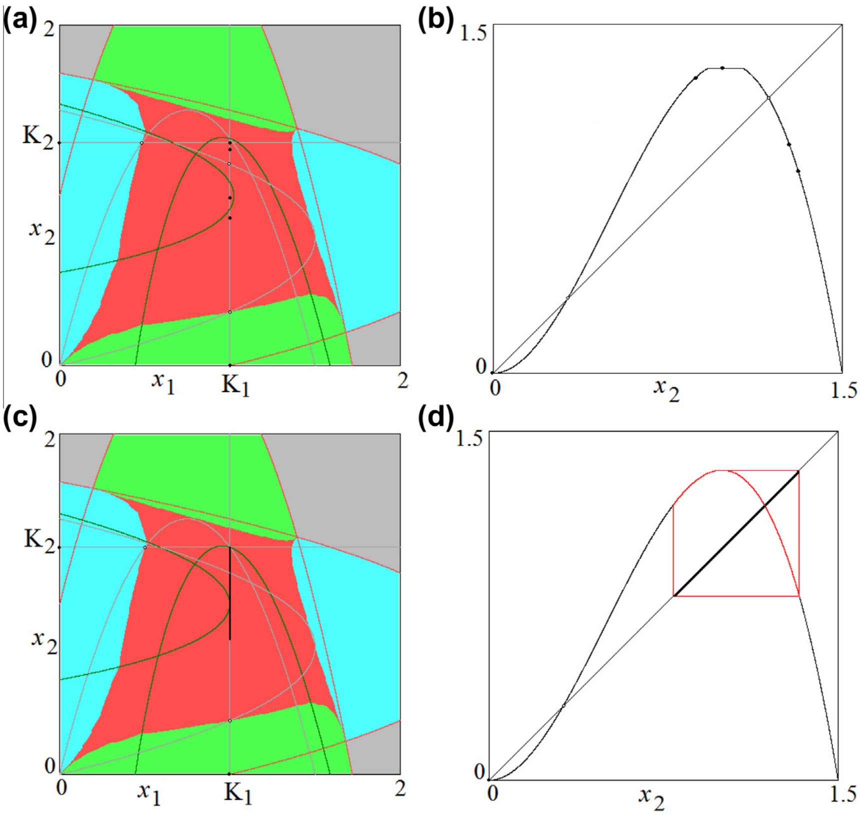

Fig. 12. $K_1 = 1$. In (a) and (b) $K_2 = 1.31$. In (a) basin of attraction of the superstable 4-cycle (lying on $x_1 = K_1$) in red. In (b) map $f_2(x_2)$ describing the dynamics of the model on the restriction $x_1 = K_1$. In (c) and (d) $K_2 = 1.335$. In (c) basin of attraction of the chaotic attractor (lying on $x_1 = K_1$) in red. In (d) map $f_2(x_2)$ which generates the chaotic attractor in (c). (For interpretation of the references to color in this figure legend, the reader is referred to the web version of this article.)

$x^*_{2,c}$, which satisfies $\frac{d}{dx_2}F_2\left(K_1, x^*_{2,c}\right) = 0$, where the first derivative is given in (23), and the value in the critical point (i.e. $\max_{x_2}\{F_2(K_1, x_2)\} = F_2\left(K_1, x^*_{2,c}\right)$). Via standard computations we get

$$x^*_{2,c} = \frac{N_2}{3} + \left[\left(\frac{N_2}{3}\right)^2 + \frac{N_2}{3\gamma_2\tau_2}(1 - \gamma_2 K_1)\right]^{1/2}$$

so that the maximum of the function $F_2(K_1, x_2)$ is given by

$$F_2\left(K_1, x^*_{2,c}\right) = \left(x^*_{2,c}\right)^2\left(2\frac{x^*_{2,c}}{N_2} - 1\right)\gamma_2\tau_2$$

Then a BCB occurs when this maximum reaches the constraint on x_2, which is the value K_2, and thus it is determined by the condition $K_2 = F_2\left(K_1, x^*_{2,c}\right)$ which leads to the following BCB curve in the parameter space:

$$BC_{p,2} : K_2 = \left(x^*_{2,c}\right)^2\left(2\frac{x^*_{2,c}}{N_2} - 1\right)\gamma_2\tau_2 \tag{32}$$

A portion of this curve is shown in Fig. 4 and in the enlargement, in Fig. 11(b).

The other BCB due to the restriction on the straight line $x_2 = K_2$ is determined similarly, considering (17) and (18), which leads to the following BCB curve in the parameter space:

$$BC_{p,1} : K_1 = \left(x^*_{1,c}\right)^2\left(2\frac{x^*_{1,c}}{N_1} - 1\right)\gamma_1\tau_1 \tag{33}$$

In Fig. 4 a portion of both bifurcation curves $BC_{p,i}$ are shown, and better visible is $BC_{p,2}$ in the enlargement in Fig. 11(b). From the two-dimensional bifurcation diagram we can see that the BCB occurring crossing the curve $BC_{e,1}$ leads to persistence, while its portion in the region with vertical strips is no longer a bifurcation, as the restriction to the one-dimensional map is smooth and the point (K_1, K_2) does not belong to the attracting set.

Differently, the crossing of the curve $BC_{p,2}$ leading to a smooth restriction, determines the transition from a piecewise-smooth (with a flat branch) to a smooth map. It is worth to note that each periodicity region associated with a superstable cycle, on the left side of the curve $BC_{p,2}$, leads to a correspondent vertical strip associated with an attracting cycle on its right side. On the left side of the curve $BC_{p,2}$ the periodicity regions of superstable cycles have as limit sets curves related with homoclinic bifurcations, which also leads to correspondent vertical lines associated with chaotic dynamics on the right side (when the map is smooth).

In order to illustrate the dynamics of T in this parameter region we consider two more paths, at $K_2 = 1.48$ and at $K_2 = 1.37$ which also are evidenced in Figs. 4 and 11(b), and describe some bifurcations occurring as K_1 increases.

Let us start considering $K_2 = 1.48$ fixed. From Fig. 11(b) we can see that increasing K_1 first the BCB crossing $BC_{e,1}$ occurs, and then the crossing of $BC_{p,2}$. The one-dimensional bifurcation diagram as a function of K_1 is shown in Fig. 13(a). In the region where the dynamics are represented by the U-sequence as commented above, the effect of the crossing of $BC_{e,1}$ (which occurs approximately at $K_1 = 0.83$) corresponds to a persistence of the attracting cycle: before the bifurcation the superstable cycles have one periodic point in the region Ω_7 and all others in the region Ω_5 while after the bifurcation the periodic point (K_1, K_2) belongs to the region Ω_1, its preimage to the region Ω_7 and all others in the region Ω_5. The attractors and related basins at $K_1 = 0.84$ are shown in Fig. 14(a). Then, increasing K_1 the crossing of $BC_{p,2}$ occurs (approximately at $K_1 = 0.855$), and this leads to a smooth shape of the first return map on $x_1 = K_1$ (as above in Fig. 12(d)). The attracting set on this line seems a large invariant chaotic interval, as shown in Fig. 14(b). Notice that after this bifurcation, the corner point (K_1, K_2) (belonging to the region Ω_1) does not belong to the attracting set. This fact may lead to changes in the structure of the basins of attraction of the attracting sets. As an example, in Fig. 14(b) the corner point is very close to the boundary separating the basin of the chaotic attractor from the basin of the fixed point $(K_1, 0)$. In Fig. 14(c) (at $K_1 = 0.9$) we are at the contact: the corner point belongs to the boundary of the basin of $(K_1, 0)$, as in fact the complete region Ω_7 which is mapped into P, now belongs to the basin of $(K_1, 0)$ together with all its preimages of any rank. Increasing K_1 the attractor (a cycle or a chaotic attractor) takes a more complex shape in the two-dimensional phase plane: the dynamics can still be studied by using the first return map on the line $x_1 = K_1$ but the number of points of a trajectory outside the line changes at each iteration so that it is difficult to have it analytically, even in implicit form (an example is shown in Fig. 14(d)). In this last figure we can see that the chaotic attractor is very close to the boundary of its basin of attraction. The contact, leading to its "final bifurcation", occurs approximately at $K_1 = 1.198$. After it is transformed into a chaotic repeller, leaving only the two attracting fixed points on the axes, with a basin of attraction having a fractal structure (similar to the one shown above in Fig. 7).

Similarly we can comment the one-dimensional bifurcation diagram as a function of K_1 shown in Fig. 13(b). From the region where the dynamics are associated with superstable cycles and the U-sequence, the BCB crossing $BC_{p,2}$ occurs approximately at $K_1 = 0.963$, leading to a chaotic attractor, which completely belongs to the line $x_1 = K_1$ even if after the bifurcation the point (K_1, K_2) no longer belongs to the attractor. Here the crossing of $BC_{e,1}$, which occurs approximately at $K_1 = 0.975$, does not represent a bifurcation, it only denotes the transition of the corner point (K_1, K_2) from region Ω_5 to the region Ω_1. Differently from the bifurcation diagram in Fig. 13(a), here increasing K_1 it can be noticed another region in which the dynamics are again described by superstable cycles in the U-sequence structure. This transition happens when the existing attractor has a contact, i.e. a border collision, with the boundary of region Ω_7. In our example this occurs approximately at $K_1 = 1.185$. After the contact the attractor is a superstable cycle with one periodic point in the region Ω_7 and thus it is mapped into $P = (K_1, K_2)$ which is again a periodic point. Now the "final bifurcation" of this attractor happens when the periodic point $P = (K_1, K_2)$ has a contact with its basin boundary, which occurs approximately at the value $K_1 = 1.245$, and on the other side of the contact point there is the basin of the fixed point $(K_1, 0)$ so that after the bifurcation the attractors are only the fixed points on the axes, and the basin of the equilibrium of segregation $(K_1, 0)$ has a huge increases.

For what concerns the implications of the entry constraints, K_1 and K_2, in terms of segregation, the analysis performed in this section reveals that the effects of these entry constraints change if we make a discrimination on the maximum number of agents allowed to enter the system between the two groups. Indeed, if the difference between K_i and K_j is sufficiently large, with K_i near to N_i and K_j small, then we will have only stable equilibria of segregation. Moreover, starting with K_i relatively large and increasing K_j, a stable equilibrium of non segregation cannot be reached, but rather an attractor in which the number of agents of the two groups that enter and exit the system fluctuates over time and when K_j becomes suf-

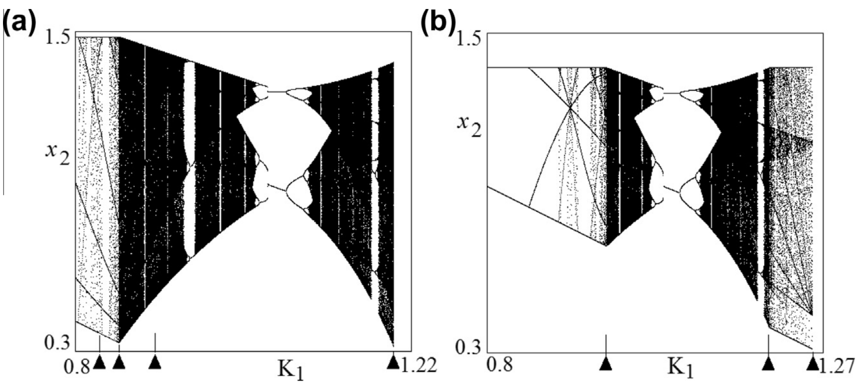

Fig. 13. 1D bifurcation diagram for $K_1 \in [0.8, 1.27]$. In (a) $K_2 = 1.48$, in (b) $K_2 = 1.37$.

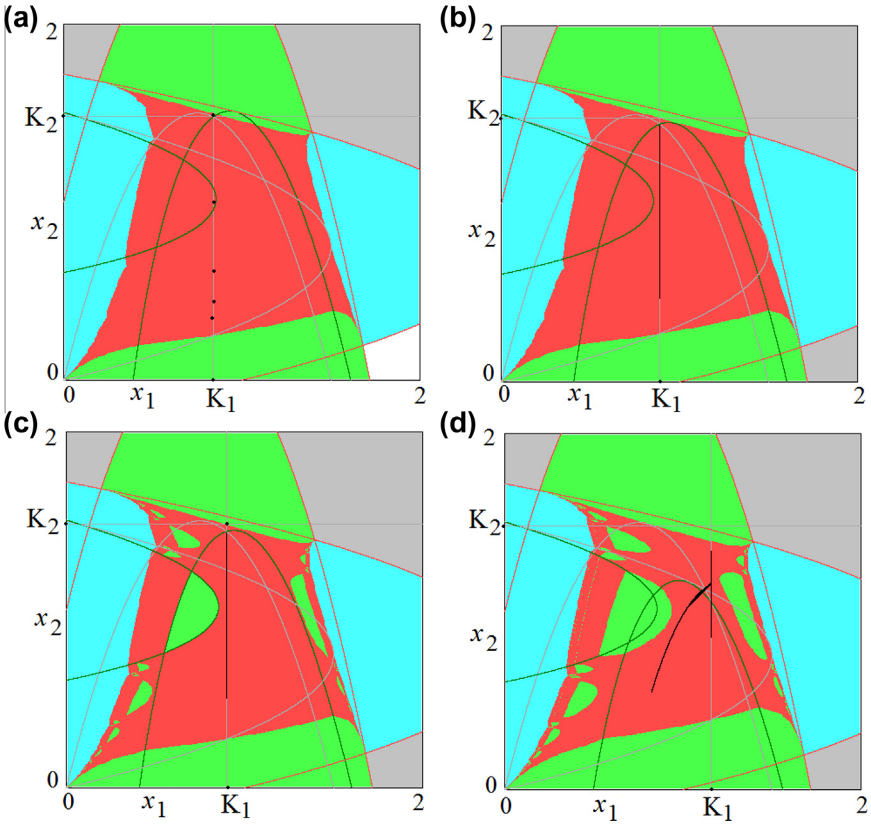

Fig. 14. $K_2 = 1.48$. In (a) basins of attraction and attractors for $K_1 = 0.84$. In (b) basins of attraction and attractors for $K_1 = 0.89$. In (c) basins of attraction and attractors for $K_1 = 0.9$, here the corner point (K_1, K_2) is marked with a black dot for highlighting that it enters the basin of attraction of $(K_1, 0)$, i.e. the green region. In (d) basins of attractions and attractors for $K_1 = 1.16$. (For interpretation of the references to color in this figure legend, the reader is referred to the web version of this article.)

ficiently large again only an equilibrium of segregation is possible. This reveals an important aspect of the issue of segregation, i.e. to avoid overreaction of the two groups toward segregation we need to limit in a similar way the number of possible entrances of both types of agents in the system.

The result that imposing sufficiently stringent entry constraints to both groups helps to avoid segregation has a straightforward interpretation if we note that to limit the maximum number of agents of each group allowed to enter the system is equivalent to exclude the less intolerant population to enter the system. Indeed, the more tolerant members are the first ones to enter the system because they do not suffer the presence of members of the other group. It follows that in a system where there are two different groups of people and only the more tolerant members of each group are allowed to enter the system the probability of avoiding segregation increases. This gives a clear indication that the forces that drive the system to segregation are the less tolerant individuals.

Another interesting aspect is related to the effect of imposing an entry constraint only on one of the two groups. This is a real common situation as in many countries the authorities tends to impose entry limitations for foreigners with the hope to avoid problems of segregation. The proposed analysis suggests that this policy could increase, instead of decreasing, the risk of segregation as the least tolerant members of the indigenous population which does not suffer entry constraints are stimulated to stay in the system preventing the creation of equilibria of non segregation.

4. Conclusions

In this work we have analyzed the effects of several constraints on the dynamics of the adaptive model of segregation proposed in [2]. The constraints represent the maximum number of agents of two different groups that are allowed to enter a system. We have provided an accurate investigation of the dynamics in the symmetric case, i.e. when the two groups of agents that differ for a specific feature are of the same size and have the same level of tolerance. The definition of the two-dimensional piecewise smooth map lead to a map with different definitions in several partitions. Besides the existence of two stable segregation equilibria on the axes, we have shown that other attractors may exist, regular or chaotic. The effect of the constraints, modifying the regions, leads to border collision bifurcations of the positive attracting sets. In the (K_1, K_2)-parameter plane of the constraints, we have determined several BCB curves, and explained their effects on the dynamic behaviors. The results are obtained by using first return maps on suitable intervals, and applying the bifurcation theory for one-dimensional piecewise smooth maps. A deep investigation of the effects of the constraints when the symmetry is broken is desirable and can reveal dynamics not observable in the symmetric setting. This line of research is left for further studies.

Many further extensions of this segregation model could be of particular interest. For example, due to empirical evidences suggesting that groups of people could have different propensity toward integration with other groups of people, see, e.g., [5], a deep analysis devoted to investigate the dynamics of the segregation model when the two groups differ for their tolerance function will provide interesting and important developments and will increase the understanding of the mechanisms that lead to or prevent segregation.

To conclude, the functions $R_i(x_i)$ used in this paper, given in (1), have been proposed as representative of the description given by Schelling in [24]. However, in the conclusions of their paper, the authors of [2] also propose a different formulation for these functions, which also deserve a deeper investigation.

Acknowledgments

V. Avrutin is supported by the European Community within the scope of the project "Multiple-discontinuity induced bifurcations in theory and applications" (Marie Curie Action of the 7th Framework Programme, Contract Agreement N. PIEF-GA-2011-300281). The other two authors have worked under the auspices of COST Action IS1104 "The EU in the new complex geography of economic systems: models, tools and policy evaluation". The authors thank Gian Italo Bischi and three anonymous referees for valuable comments and remarks. The usual caveats apply.

References

[1] Bischi GI, Gardini L, Merlone U. Impulsivity in binary choices and the emergence of periodicity. Discrete Dyn Nat Soc 2009;2009. http://dx.doi.org/10.1155/2009/407913. Article ID 407913, 22 pages.
[2] Bischi GI, Merlone U. Nonlinear economic dynamics. An adaptive dynamic model of segregation. New York: Nova Science Publisher; 2011. chapter, p. 191–205.
[3] Brianzoni S, Michetti E, Sushko I. Border collision bifurcations of superstable cycles in a one-dimensional piecewise smooth map. Math Comput Simul 2010;81(1):52–61.
[4] Bischi GI, Chiarella C, Kopel M, Szidarovszky F. Nonlinear oligopolies: stability and bifurcations. Heidelberg: Springer; 2010.
[5] Clark WAV. Residential preferences and neighborhood racial segregation: a test of the schelling segregation model. Demography 1991;28(1):1–19.
[6] Dal Forno A, Gardini L, Merlone U. Ternary choices in repeated games and border collision bifurcations. Chaos Solitons Fract 2012;45(3):294–305.
[7] Day R. Complex economic dynamics. Cambridge: MIT Press; 1994.
[8] Day R, Chen P. Nonlinear dynamics and evolutionary economics. Chaotically switching bear and bull markets: the derivation of stock price distributions from behavioral rules. Oxford: Oxford University Press; 1993. chapter, p. 169–82.
[9] di Bernardo M, Budd CJ, Champneys AR, Kowalczyk P. Piecewise-smooth dynamical systems: theory and applications. Berlin: Springer-Verlag; 2008.
[10] Epstein JM, Axtell R. Growing artificial societies: social science from the bottom up. Washington, DC: Brookings Inst. Press; 1996.
[11] Futter B, Avrutin V, Schanz M. The discontinuous flat top tent map and the nested period incrementing bifurcation structure. Chaos Solitons Fract 2012;45(4):465–82.
[12] Gardini L, Merlone U, Tramontana F. Inertia in binary choices: continuity breaking and big-bang bifurcation points. J Econ Behav Organiz 2011;80(1):153–67.
[13] Gardini L, Sushko I, Naimzada A. Growing through chaotic intervals. J Econ Theory 2008;143:541–57.
[14] Hao BL. Elementary symbolic dynamics and chaos in dissipative systems. Singapore: World Scientific; 1989.
[15] Hommes C, Nusse H. Period three to period two bifurcation for piecewise linear models. J Econ 1991;54(2):157–69.
[16] Ito S, Tanaka S, Nakada H. On unimodal transformations and chaos II. Tokyo J Math 1979;2:241–59.
[17] Matsuyama K. The good, the bad, and the ugly: an inquiry into the causes and nature of credit cycles. Center for Mathematical Studies in Economics and Management. Science Discussion Paper No.1391, Northwestern University; 2011.
[18] Maštrenko Yu L, Maštrenko VL, Chua LO. Cycles of chaotic intervals in a time-delayed Chua's circuit. Int J Bifur Chaos Appl Sci Eng 1993;3(6):1557–72.
[19] Metropolis N, Stein ML, Stein PR. On finite limit sets for transformations on the unit interval. J Comb Theory 1973;15:25–44.
[20] Nusse HE, Yorke JA. Border-collision bifurcations including period two to period three for piecewise smooth systems. Physica D 1992;57(1–2):39–57.
[21] Nusse HE, Yorke JA. Border-collision bifurcations for piecewise smooth one-dimensional maps. Int J Bifur Chaos Appl Sci Eng 1995;5(1):189–207.
[22] Puu T, Sushko I. Oligopoly dynamics, models and tools. New York: Springer Verlag; 2002.
[23] Puu T, Sushko I. Business cycle dynamics, models and tools. New York: Springer Verlag; 2006.
[24] Schelling TC. Models of segregation. Am Econ Rev 1969;59(2):488–93.
[25] Schelling TC. Dynamic models of segregation. J Math Sociol. 1971;1(1):143–86.
[26] Sushko I, Agliari A, Gardini L. Bifurcation structure of parameter plane for a family of unimodal piecewise smooth maps: border-collision bifurcation curves. Chaos Solitons Fract 2006;29(3):756–70.
[27] Sushko I, Gardini L. Degenerate bifurcations and border collisions in piecewise smooth 1d and 2d maps. Int J Bifur Chaos 2010;20:2045–70.
[28] Sushko I, Gardini L, Matsuyama K. Superstable credit cycles and U-sequence. Chaos Solitons Fract 2014;59:13–27.
[29] Tramontana F, Gardini L, Puu T. Mathematical properties of a combined Cournot–Stackelberg model. Chaos Solitons Fract 2011;44:58–70.
[30] Tramontana F, Gardini L, Westerhoff F. Heterogeneous speculators and asset price dynamics: further results from a one-dimensional discontinuous piecewise-linear map. Comput Econ 2011;38(3):329–47.
[31] Tramontana F, Westerhoff F, Gardini L. On the complicated price dynamics of a simple one-dimensional discontinuous financial market model with heterogeneous interacting traders. J Econ Behav Organiz 2010;74(3):187–205.
[32] Zhang J. Residential segregation in an all-integrationist world. J Econ Behav Organiz 2004;54:533–50.
[33] Zhusubaliyev ZT, Mosekilde E. Bifurcations and chaos in piecewise-smooth dynamical systems. River Edge, NJ: World Scientific; 2003.